PCCP

ARTICLE TYPE

Cite this: DOI: 00.0000/xxxxxxxxxx

Supplementary Material: Superfluid helium droplet-mediated surface-deposition of neutral and charged silver atomic species†

Berta Fernández,[a] Martí Pi,[b,c] and María Pilar de Lara-Castells*[d]

1 Extra details for the evaluated *ab initio* intermolecular potentials.

1.1 Intermolecular Ag–graphene potentials

The intermolecular Ag–graphene potential has been calculated using the periodic dlDF + incremental D^*_{as} scheme,[1,2] combining the dispersionless density functional dlDF[3] with the coupled cluster singles and doubles with perturbative triple corrections, CCSD(T), method for the dispersion interaction. The periodic dlDF calculations were carried out using the same computational set-up reported in Ref. 2 for the Ag_2–graphene interaction using a modified version of the CRYSTAL code[4] including the implementation of the dlDF approach.[1] Very briefly, we used a 3 × 3 graphene supercell model with the aug-cc-pVDZ basis set on carbon atoms. The relativistic small-core Ag pseudopotential of Andrae et al.[5] was also used together with the corresponding basis set as modified for CRYSTAL calculations by Doll and Harrison.[6] The Brillouin-zone integrations were carried out using a Monkhorst-Pack grid[7] 12×12. Structural relaxation effects of the carbon atom positions were not accounted for since we verified their negligible effect on Density Functional Theory (DFT) calculations.

Within the incremental D^*_{as} scheme, the *intermonomer* correlation contribution to the correlation energy calculated at CCSD(T) level[2] is identified with the dispersion contribution, fitted by means of the effective pairwise D_{as} functional of Szalewicz and collaborators,[8,9] and then computed on the extended system. For Ag–graphene, the calculation of the interaction energy $E^{\rm total}_{\rm int}$ is then reduced to,

$$E^{\rm tot}_{\rm int} = E^{\rm dlDF}_{\rm int} - \sum_{\rm C}\sum_{n=6,8} \frac{\sqrt{C^{\rm Ag}_n C^{\rm C}_n}}{R^n_{\rm AgC}} f_n\left(\sqrt{\beta_{\rm Ag}\beta_{\rm C}} R_{\rm AgC}\right),$$

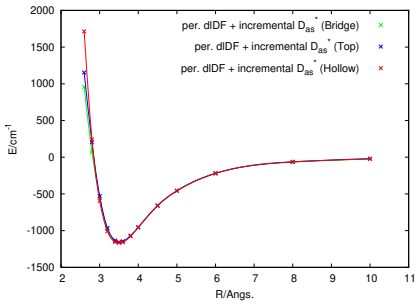

Fig. 1 Ag–graphene interaction potential as function of the distance between the Ag atom and different positions (hollow, bridge, and top) onto the graphene sheet. The periodic dlDF + incremental D^*_{as} scheme[1,2] has been used.

where the sum in the second term (the D_{as} function) runs over as many graphene C atoms as necessary to get convergence and f_n are the damping functions of Tang and Toennies.[10] As analyzed in previous works,[1,2,11] the efficiency and accuracy of this scheme relies on the size and transferability properties of the surface cluster used to fit the *intermonomer* correlation. In this work, we have applied the parametrization reported in Ref. 2 from CCSD(T) calculations for the Ag_2–coronene system. The coefficients for this parametrization have been previously provided in Table S1 of the Supporting Information of Ref. 12. Our results in the present work for different adsorption positions (hollow, top, and bridge) are depicted in Figure 3.

1.2 Assessment of the accuracy of the dlDF + incremental D^*_{as} scheme

The accuracy of the dlDF + incremental D^*_{as} scheme was tested for the Ag–coronene complex through comparison with the benchmark calculations reported in Ref. 13, getting an agreement to within 3% for the interaction energy at the potential minimum (-1375.4 cm^{-1}, see Figure 2). Our dlDF calculations of the Ag–coronene interactions were carried out using the MOLPRO code.[14] Based on their proven good performance on supported Ag_2 clusters,[2] the atom-centered (augmented) polarized correlation-consistent triple-ζ aug-cc-pVTZ-PP basis set (denoted as aVTZ) has been chosen,[15] including a small (10-valence-electron) relativistic pseudo-potential. The benchmark value in Ref. 13 was

[a] Department of Physical Chemistry. University of Santiago de Compostela. E-15782 Santiago de Compostela, Spain.
[b] Departament FQA, Facultat de Física, Universitat de Barcelona, Diagonal 645, 08028 Barcelona, Spain.
[c] Institute of Nanoscience and Nanotechnology (IN2UB), Universitat de Barcelona, 08028 Barcelona, Spain.
[d] Institute of Fundamental Physics (AbinitSim Unit), Madrid, Spain. E-mail: Pilar.deLara.Castells@csic.es

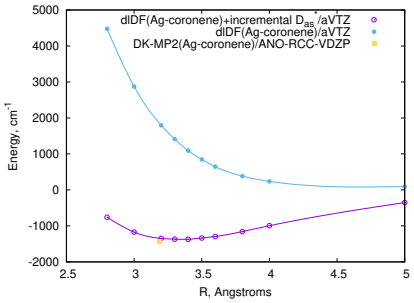

Fig. 2 Ag–coronene interaction potential as function of the distance between the Ag atom and the hollow position onto coronene. The periodic dlDF + incremental D_{as}^{*} scheme[1,2] has been used. The best benchmark values for the interaction energy and the Ag–coronene equilibrium distance at the potential minimum, as reported in Ref. 13, are also indicated.

obtained using the scalar one-component Douglas–Kroll–Hess approximation[16] in relativistic MP2 calculations with ANO-RCC basis sets,[17,18] containing diffuse and polarization functions. As mentioned in Ref. 13, the DK-MP2 method along with the double-ζ ANO-RCC-VDZP basis set yielded similar interaction energies to that obtained CCSD(T) with the ANO-RCC-VTZP basis for the Ag-benzene interaction. However, the MP2 calculations including larger basis (triple-η) basis sets overestimated the interaction energies. Similarly, as reported in Ref. 19, MP2 calculations with a double-ζ basis set closely followed those obtained at CCSD(T) with a triple-ζ basis set for the Cs_2–benzene interaction. This way, as reported in this work for the case of the Ag^+–coronene interaction, the use of a smaller basis set in MP2 calculations compensate its over-estimation of the interaction energies. As discussed in Ref. 13, the Ag–coronene and Ag–graphene interactions are dispersion-dominated so that the dlDF interaction energies are overly repulsive (see Figure 2). It can also be observed in Figure 1 that they depend very slightly on the particular adsorption position in the graphene sheet (see also Ref. 13).

1.3 Intermolecular Ag^+– He and Ag^+–graphene potentials

The second step in our investigation was the evaluation of the Ag^+– He complex interaction potential. Our third aim was to simulate the interaction between Ag^+ and graphene and bearing in mind the large size of the latter, we considered complexes formed by hydrocarbons of increased size starting with the Ag^+– benzene potential, and from there we enlarged the hydrocarbon in a systematic way, evaluating interaction energies for Ag^+– coronene and the Ag^+– circumpyrene. We expect the latter results to be able to give insight into the interaction of Ag^+ with larger similarly extended hydrocarbons, by providing an interaction potential that can be considered converged with respect to molecular size.

The interaction potentials were evaluated using the supermolecular model and counterpoise corrected for basis set superposition error. In this way, the interaction energies were obtained as the difference between the complex energy and the sum of the monomer energies and all the three energies were calculated in the complex basis set. In all cases the monomer geometries were kept fixed during the calculations, since it is a good approximation to consider changes in intramolecular geometries negligible in evaluations of intermolecular energies. The molecular geometries for benzene and circumpyrene were obtained from the literature and that of coronene was evaluated at the DFT(PBE-D3)/6-31G** level of theory.

Considering the increase in size of the complexes we are trying to model, we need to bear in mind the use of Density Functional Theory (DFT) to be able to evaluate the potentials for the systems where 'ab initio' methods are too demanding. Therefore, in all cases but the Ag^+– He complex we carried out DFT interaction energy calculations. For comparison purposes, the dispersion-corrected DFT-D3(BJ) *ansatz* has been chosen,[20,21] given its good performance in describing the adsorption of the silver dimer (Ag_2) on graphene.[2] Specifically, this scheme consists in applying the Perdew-Burke-Ernzerhof (PBE) density functional[22] and the Becke-Johnson (BJ) damping[20] for the D3 dispersion correction.

Based on previous benchmarking on the adsorption of the Ag_2 dimer on benzene and coronene,[2] atom-centered (augmented) polarized correlation-consistent [(aug)-cc-pVXZ(-PP), X=2–6) basis sets have been chosen, including a small (10-valence-electron) relativistic pseudopotential for Ag^+. For the Ag^+–He complex and due to the reduced size of the complex, we evaluated the interaction potential using the coupled cluster singles and doubles with perturbative triple corrections, CCSD(T), method and two sets of bases: the first set consisted in the aug-cc-pVQZ-PP basis set for the Ag^+ and the aug-cc-pV5Z for He (denoted 45 in the following) and for the second one the aug-cc-pV5Z-PP basis set was used for the Ag^+ cation and the aug-cc-pV6Z for the He atom (denoted 56). The corresponding potentials were extrapolated to complete basis set limit (CBS).

In the case of the Ag^+– benzene complex we carried out calculations for the potential curve along the line perpendicular to the benzene plane and passing through the benzene center of mass. We selected this potential curve, because in benzene – atom complexes the absolute minima of the intermolecular potential energy surface lie on it. The interaction energies were evaluated at the CCSD(T) level using the aug-cc-pVDZ basis set for the C and H atoms, and the aug-cc-pVDZ-PP basis set for Ag^+ extended with a set of 3s3p2d1f1g midbond functions (denoted aVDZmb in the following). These functions are well known to improve convergence of the interaction energies with respect to basis set limit. The midbond functions are placed in the middle of the line joining the cation and the center of mass of the molecule and have exponents of 0.9, 0.3, and 0.1 for the s and the p functions, 0.6 and 0.2 for the d functions, and 0.3 for the f and g functions. The CCSD(T) results were considered as benchmark in the following. Bearing in mind the extension of our study to interaction potentials of Ag^+ with larger hydrocarbons, we additionally evaluated the potential at the MP2 level and with aug-cc-pVDZ (for C and H) and the aug-cc-pVDZ-PP for Ag^+ bases (denoted aVDZ basis set), this time without the set of midbond functions. The combination of the aug-cc-pVDZ basis set and the MP2 correlation treatment was proven in the literature to be an efficient way of getting close to CCSD(T)/aVDZmb quality results. We also tested the performance of the DFT method together with the PBE functional, the

aVDZmb basis set, and correcting with the D3 dispersion term (denoted PBE-D3 method in the following).

For the Ag^+– coronene and the Ag^+– circumpyrene complexes we evaluated the interaction energies along the axis that crosses the hydrocarbon center of mass and is perpendicular to the plane of the molecule in the case of coronene and perpendicular to the central C-C bond and on the concave side of the molecule for the circumpyrene. In a similar way to the Ag^+– benzene case we used the MP2/aVDZ and the DFT(PBE-D3)/aVDZmb levels of theory. All electronic structure calculations have been carried out with the ORCA suite of programs[23–25] (version 5.0.1), while the Avogadro and the Gnuplot codes were used for geometry and interaction potential representations, respectively.

2 Extended results and discussion

The obtained results are summarized in Figures 1 to 3 and in Figure 2 and Table 1 in the manuscript.

Figure 2 in the manuscript displays the Ag^+– He complex interaction potential, evaluated at the CCSD(T) level using the 45 and 56 bases. Extrapolated CBS–limit results are also displayed. The potential evaluated with the 45 basis set differs in 14 cm^{-1} (.04 kcal/mol) from the CBS result, underestimating the interaction (see Table 1). The corresponding difference in the distance at the minimum is .0091 Å. These discrepancies get much smaller when extending the basis set to the 56 level, i.e. 2.8 cm^{-1} (.01 kcal/mol) and .0018 Å . Taking into account the pursued accuracy, we can consider the 56 values converged with respect to basis set extension.

The main potentials obtained for the Ag^+– benzene complex, i.e. those evaluated at the DFT(PBE-D3)/aVDZmb, MP2/aVDZ, and CCSD(T)/aVDZmb levels, are plotted in Figure 1. The DFT potential clearly overestimates the atraction with respect to the other two potentials. Additionally, at long range (distances larger than 8 Å) it does not simulate the behaviour of the interaction, by not systematically increasing the interaction energy towards zero at dissociation limit. The MP2 and coupled cluster potentials lie close to each other, with differences negligible for our purposes in the present study. To get more insight into this, in Table 1 we compare the interaction potential minima for the Ag^+– benzene complex obtained with the used methodologies. There are differences between the PBE/aVDZmb and the 'ab initio' MP2/aVDZ values in the order of 1539 cm^{-1} (4.400 kcal/mol) in the interaction energy and of .0206 Å in the distance at the minima. The MP2/aVDZmb approach provides a potential 176 cm^{-1} (.503 kcal/mol) deeper than the CCSD(T)/aVDZmb, and with a shorter minimum distance (by .0265 Å), therefore only slightly resulting in a stronger interaction. For this complex we also carried out calculations using the domain based local pair natural orbital CCSD(T) method (DLPNO-CCSD(T)) together with the aVDZmb basis set. The DLPNO-CCSD(T) approach interaction energy minimum is included in Table 1. DLPNO-CCSD(T) overestimates the interaction strength by 473 cm^{-1} (1.35 kcal/mol) when compared to the corresponding energy evaluated at the CCSD(T)/aVDZmb level. Additionally, the Ag^+– benzene distance at the lowest energy points results 0.1027 Å shorter than the reference value.

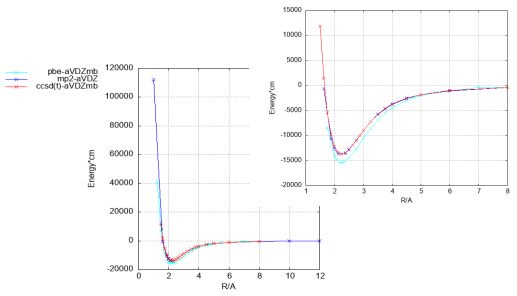

Fig. 3 Ag^+– benzene complex interaction potential, evaluated at the CCSD(T), MP2 and DFT(PBE-D3) levels with aug-cc-pVDZ basis sets. In the CCSD(T) and DFT calculations the bases were extended with a set of midbond functions. See text for further details.

Table 1 Potential minima obtained with the different methodologies. Distance between the cation and the center of mass of the molecule, R, in Å and interaction energies in cm^{-1}. See text for further details.

Complex	Method/basis set	R	Energy
Ag^+– He	CCSD(T)/45	2.4100	−392.8
	CCSD(T)/56	2.4027	−403.9
	CCSD(T)/CBS	2.4009	−406.7
Ag^+– benzene	PBE/aVDZmb	2.2513	−15424.6
	MP2/aVDZ-NoCP	2.1625	−17132.2
	MP2/VDZ-NoCP	2.2095	−14358.5
	MP2/aVDZ	2.2307	−13885.6
	CCSD(T)/aVDZmb	2.2572	−13709.6
	DLPNO-CCSD(T)/aVDZmb	2.1545	−14182.4
Ag^+– coronene	PBE/aVDZmb	2.2503	−18097.2
	MP2/aVDZ	2.1924	−17085.3
Ag^+– circumpyrene	PBE/aVDZmb	2.3626	−22802.4
	MP2/aVDZ	2.1900	−17500.5

From the above results, we concluded that the MP2/aVDZ combination provided an efficient methodology to reproduce the CCSD(T)/aVDZmb potential in the case of the Ag^+– benzene complex, being the errors within the aimed accuracy in the present investigation. The MP2 method is well known to overestimate interaction strengths, but when used together with the aVDZ basis set, the mentioned overestimation if partially cancelled out by the lack of midbond functions in the basis set. Considering the above, we expect MP2/aVDZ to also be an efficient method/basis set solution for studying similar larger molecule complexes and we selected this methodology as reference for the simulations in the extended complexes.

Since the DFT(PBE-D3)/aVDZmb results could not reproduce the 'ab initio' potentials for the benzene, coronene and circumpyrene complexes, providing significant discrepancies in the region around the minima – larger interaction energies, considerably overestimating the strength of the interaction, and predicting too long equilibrium distances (see Table 1)– and behaving differently at larger distances towards the dissociation limit, we will not consider these results any further in the analysis. We checked that the incorrect large distance results were not due to basis set deficiencies, by carrying out calculations with larger bases at particularly problematic distances.

The MP2/aVDZ results for the Ag^+– coronene and Ag^+– circumpyrene complexes are displayed in Figure 4 Figure 5, respectively, and in Table 1.

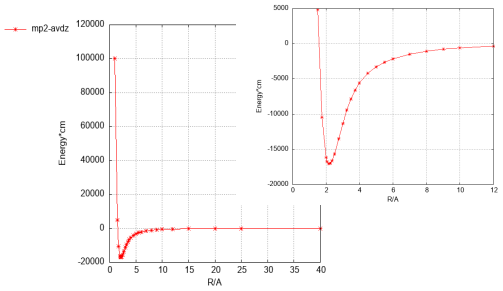

Fig. 4 Ag^+– coronene complex interaction potential, evaluated at the MP2 level with aVDZ basis sets. See text for further details.

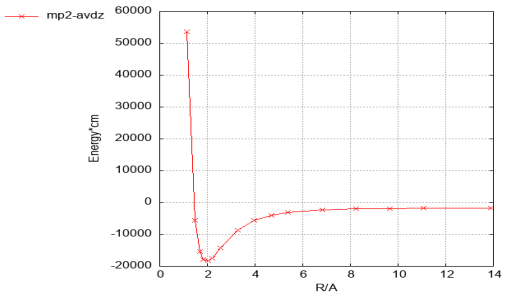

Fig. 5 Ag^+– circumpyrene complex interaction potential, evaluated at the MP2 level with the aVDZ bases. See text for further details.

There are differences in interaction energies in the order of 1012 and 5302 cm^{-1} (2.89 and 15.16 kcal/mol) between the PBE/aVDZmb and the 'ab initio' MP2/aVDZ values for Ag^+– coronene and Ag^+– circumpyrene, respectively. The corresponding discrepancies in the distances at the minima are .0579 and .1726 Å , respectively (see Table 1).

All the evaluated MP2/aVDZ potential curves are compared in Figure 2 in the manuscript and in Table 1. The differences between the Ag^+– benzene and the other two potentials are considerable, both at the equilibrium and long range regions. In this way, at the minimum the former potential is 3614.9 cm^{-1} (10.3 kcal/mol) shallower and the equilibrium distance is 0.0407 Å longer than those of the Ag^+– circumpyrene complex. Nevertheless, when comparing the Ag^+– coronene and Ag^+– circumpyrene potentials, the differences between these two potentials are considerably smaller, being the former potential 415.2 cm^{-1} (1.2 kcal/mol) shallower and the equilibrium distance 0.0024< Å longer than those for the latter complex. With these small differences, we can consider that the intermolecular potentials are converged with respect to the size of the hydrocarbon modelling a single graphene sheet.

Notes and references

1 M. P. de Lara-Castells, H. Stoll, B. Civalleri, M. Causà, E. Voloshina, A. O. Mitrushchenkov and M. Pi, *J. Chem. Phys.*, 2014, **141**, 151102.

2 M. P. de Lara-Castells, A. O. Mitrushchenkov and H. Stoll, *J. Chem. Phys.*, 2015, **143**, 102804.

3 K. Pernal, R. Podeszwa, K. Patkowski and K. Szalewicz, *Phys. Rev. Lett.*, 2009, **103**, 263201.

4 R. Dovesi, V. R. Saunderds, C. Roetti, R. Orlando, C. M. Zicovich-Wilson, F. Pascale, B. Civalleri, K. Doll, N. M. Harrison, I. J. Bush, P. D'Arco, M. Llunel, M. Causà and Y. Noël.

5 D. Andrae, U. Haüssermann, M. Dolg, H. Stoll and H. Preuss, *Theor. Chim. Acta*, 1990, **77**, 123.

6 K. Doll and N. M. Harrison, *Phys. Rev. B*, 2001, **63**, 165410.

7 H. J. Monkhorst and J. D. Pack, *Phys. Rev. B*, 1976, **13**, 5188–5192.

8 R. Podeszwa and K. Szalewicz, *J. Chem. Phys.*, 2012, **136**, 161102.

9 R. Podeszwa, K. Pernal, K. Patkowski and K. Szalewicz, *J. Phys. Chem. Lett.*, 2010, **1**, 550–555.

10 K. T. Tang and J. P. Toennies, *J. Chem. Phys.*, 1984, **80**, 3726–3741.

11 M. P. de Lara-Castells, H. Stoll and A. O. Mitrushchenkov, *J. Phys. Chem. A*, 2014, **118**, 6367–6384.

12 R. Fernández-Perea, L. F. Gómez, C. Cabrillo, M. Pi, A. O. Mitrushchenkov, A. F. Vilesov and M. P. de Lara-Castells, *J. Phys. Chem. C*, 2017, **121**, 22248–22257.

13 J. Granatier, P. Lazar, M. Otyepka and P. Hobza, *J. Chem. Theory Comput.*, 2011, **7**, 3743–3755.

14 H.-J. Werner, P. J. Knowles, F. R. Manby, J. A. Black, K. Doll, A. Heßelmann, D. Kats, A. Köhn, T. Korona, D. A. Kreplin, Q. Ma, T. F. Miller, A. Mitrushchenkov, K. A. Peterson, I. Polyak, G. Rauhut and M. Sibaev, *J. Chem. Phys.*, 2020, **152**, 144107.

15 D. Figgen, G. Rauhut, M. Dolg and H. Stoll, *Chem. Phys.*, 2005, **311**, 227–244.

16 M. Douglas and N. M. Kroll, *Ann. Phys.*, 1974, **82**, 89–155.

17 B. O. Roos, R. Lindh, P.-A. Malmqvist, V. Veryazov and P.-O. Widmark, *J. Phys. Chem. A*, 2004, **108**, 2851–2858.

18 B. O. Roos, R. Lindh, P.-A. Malmqvist, V. Veryazov and P.-O. Widmark, *J. Phys. Chem. A*, 2005, **109**, 6575–6579.

19 M. P. de Lara-Castells, A. W. Hauser and A. O. Mitrushchenkov, *J. Phys. Chem. Lett.*, 2017, **8**, 4284–4288.

20 S. Grimme, S. Ehrlich and L. Goerigk, *J. Comp. Chem.*, 2011, **32**, 1456–1465.

21 S. Grimme, J. Antony, S. Ehrlich and H. Krieg, *J. Chem. Phys.*, 2010, **132**, 154104.

22 J. P. Perdew, K. Burke and M. Ernzerhof, *Phys. Rev. Lett.*, 1996, **77**, 3865–3868.

23 F. Neese, *WIREs Computational Molecular Science*, 2012, **2**, 73–78.

24 F. Neese, *Wiley Interdiscip. Rev.: Comput. Mol. Sci.*, 2018, **8**, e1327.

25 F. Neese, *WIREs Computational Molecular Science*, 2022, **12**, e1606.

Table 2 Ag^+– He CCSD(T) interaction energies in cm^{-1}: 45, 56 and extrapolated (BSL). R is the distance between Ag^+ and He. See text for further details.

R/Å	45	56	BSL
2.0	200.6156139900557	174.0583058651585	167.587029340819
2.05	11.9383224983228	−11.742770604161766	−17.513193613304765
2.1	−126.77271630420984	−147.93555750472788	−153.0923526439479
2.15	−226.64135456214024	−245.59869520702836	−250.21807127113186
2.2	−296.43077531157974	−313.4534470961987	−317.60139822826653
2.25	−343.0438946116794	−358.36497957777397	−362.09830138140774
2.3	−371.91073426481023	−385.784822999372	−389.16555211176285
2.35	−387.34045917852734	−399.85051308413557	−402.8988648891022
2.4	−392.62782249185625	−403.94042281671733	−406.6969885261342
2.45	−390.3720622436497	−400.65927710002967	−403.1659849217655
2.5	−382.6654300858047	−392.0251451553791	−394.30584710451456
2.55	−371.09143546892346	−379.63448544638123	−381.716188851914
2.6	−356.86838207517235	−364.70406531638844	−366.61340314432533
2.65	−340.9593245732476	−348.0283829324782	−349.75091562269427
2.7	−324.0319047827134	−330.50333372276447	−332.0802407640102
2.75	−306.73357286505507	−312.71381758697	−314.1710367108635
2.8	−289.41153769952814	−294.8681159476795	−296.1977321329652
2.85	−272.36889373001634	−277.3812553309365	−278.6026282881274
2.9	−255.8303829838568	−260.3109575590705	−261.402748825255
2.95	−239.89608589583423	−244.10297560750283	−245.12807749296405
3.0	−224.69834566719038	−228.67983492757747	−229.6500129991456
3.1	−196.70479556276968	−200.06780531396151	−200.8872771501756
3.2	−171.97066318750046	−174.61182087908338	−175.25539746772853
3.4	−131.64878416148855	−133.41270175845267	−133.84251936204487
3.6	−101.61872896141728	−102.72597847190742	−102.99578434719129
3.8	−79.29311117631563	−79.9763356981409	−80.14281849030296
4.0	−62.624451974226425	−63.061864909508934	−63.168450262445454
4.2	−50.11834860955598	−50.37623130018803	−50.43907013137048
4.4	−40.57866434398798	−40.74019766515018	−40.77955883775922
4.6	−33.219899469947265	−33.3270030952276	−33.3531012664989
4.8	−27.47624840724718	−27.551967151797808	−27.570417701520636
5.0	−22.935537787502142	−22.994137505110352	−23.008416624632087
5.2	−19.31508428961393	−19.356784466623843	−19.36694563865513
5.4	−16.387951149023245	−16.421530764538588	−16.42971318184379
5.6	−14.003359295115182	−14.031452045596135	−14.038297466669556
5.8	−12.044109270450999	−12.067373575845922	−12.073042439295833
6.0	−10.4217528073196	−10.440847097810815	−10.445499844739217
7.0	−5.445823994582589	−5.457017199396994	−5.459744671744979
8.0	−3.1292692747813007	−3.141120906756572	−3.144008819470315
9.0	−1.935766233509939	−1.9441062729665197	−1.9461385083607703
10.0	−1.2652712408880602	−1.2731723249079443	−1.2750975990846134
11.0	−0.8653884668345517	−0.8730700770834733	−0.8749418716132197
12.0	−0.6143094887359808	−0.622210575289989	−0.6241358500841536

Table 3 Ag^+– benzene MP2/aug-cc-pVDZ interaction energies in cm^{-1}. R is the distance between Ag^+ and the benzene center of mass.See text for further details.

R/Å	Interaction Energy/cm^{-1}
1.0	112399.97481961717
1.625	−612.4973079829866
1.875	−10548.794617065043
2.0	−12700.882010949541
2.125	−13692.612593117636
2.25	−13879.1025126613
2.375	−13525.434739434018
2.5	−12830.20992662267
2.625	−11939.945503866753
2.875	−9962.197730955584
3.0	−8994.74218830818
3.25	−7250.7702651379495
3.5	−5817.112125024475
3.75	−4680.734119144061
4.0	−3796.0381325036064
4.5	−2584.205634198479
5.0	−1845.6989854795816
6.0	−1048.759336633246
8.0	−435.5114203726356
10.0	−220.25127741058137
12.0	−126.05833933240281

Table 4 Ag^+– coronene MP2/aug-cc-pVDZ interaction energies in cm^{-1}. R is the distance between Ag^+ and the coronene center of mass. See text for further details.

R/Å	Interaction Energy/cm^{-1}
1.0	100109.75547780057
1.5	4801.634825281847
1.75	−10430.766309252205
2.0	−16144.655285009661
2.07	−16734.050173699
2.15	−17043.25151404127
2.25	−17007.379231624484
2.35	−16628.88106268641
2.5	−15649.152539124956
2.75	−13520.33524307174
3.0	−11348.534412104565
3.25	−9435.563001993047
3.5	−7858.17973484651
3.75	−6597.391008934095
4.0	−5603.369747892693
4.5	−4193.022322060236
5.0	−3266.2299142656384
5.5	−2616.0958005673215
6.0	−2135.0644980286206
7.0	−1477.5800176188798
8.0	−1062.0080767532968
9.0	−786.1821362792466
10.0	−596.3240183911978
12.0	−364.1120981390369
15.0	−194.8679730862452
20.0	−84.9056926594498
25.0	−44.019843933341825
40.0	−10.832764902281198

Table 5 Ag^+– circumpyrene MP2/aug-cc-pVDZ interaction energies in cm^{-1}. R is the distance between Ag^+ and the circumpyrene center of mass. See text for further details.

R/Å	Interaction Energy/cm^{-1}
1.1327700276445543	53742.98977504687
1.4877722515930811	−5574.238913365458
1.7007743068176142	−15465.5003683689
1.842775861598867	−17831.8406242009
2.0273780448606855	−18362.4394971523
2.1977801859997608	−17500.50872967752
2.552784926752632	−14297.229551461083
3.2627951137057045	−8658.918812179047
3.9728058210024058	−5615.389551883002
4.682816811958563	−3986.18213082156
5.392827974535747	−3042.53831037468
6.812850599924352	−2289.3407004429437
8.232873453008581	−2008.4733137828243
9.652896433300569	−1868.231526811421
11.072919491859853	−1798.1159858357776
13.912965747920335	−1760.1956800776336